JAES | JOURNAL OF APPLIED ENGINEERING SCIENCE | www.engineeringscience.rs
ISTRAŽIVANJA I PROJEKTOVANJA ZA PRIVREDU

Indexed by

FLEXURAL STRENGTH AND DUCTILITY OF ULTRA HIGH-PERFORMANCE CEMENT-BASED COMPOSITES (UHP-CC)

Lubna Salim Danha
Department of Civil Engineering, University of Technology-Iraq, Baghdad, Iraq

Marawan Mohammed Hamid
Department of Civil Engineering, University of Technology-Iraq, Baghdad, Iraq

Aseel Abdulazeez Abdulridha
Department of Civil Engineering, University of Technology-Iraq, Baghdad, Iraq

Zinah Asaad Abdul-Husain
Department of Civil Engineering, University of Technology-Iraq, Baghdad, Iraq

Key words: *flexural tensile strength, ultra-high performance, steel fiber, strain hardening, ductility*
doi:10.5937/jaes0-32264

Cite article:

Salim Danha L., Mohammed Hamid M., Abdulazeez Abdulridha A., Asaad Abdul-Husain Z. (2022) FLEXURAL STRENGTH AND DUCTILITY OF ULTRA HIGH-PERFORMANCE CEMENT-BASED COMPOSITES (UHP-CC), *Journal of Applied Engineering Science*, 20(1), 131 - 136, DOI:10.5937/ jaes0-32264

Online aceess *of full paper is available at: www.engineeringscience.rs/browse-issues*

Istraživanja i projektovanja za privredu
Journal of Applied Engineering Science

Original Scientific Paper

doi:10.5937/jaes0-32264

Paper number: 20(2022)1, 912, 131-136

FLEXURAL STRENGTH AND DUCTILITY OF ULTRA HIGH-PERFORMANCE CEMENT-BASED COMPOSITES (UHP-CC)

Lubna Salim Danha, Marawan Mohammed Hamid, Aseel Abdulazeez Abdulridha*, Zinah Asaad Abdul-Husain

Department of Civil Engineering, University of Technology-Iraq, Baghdad, Iraq

It has been known that concrete is weak in tension, so it requires some additional materials to have ductile behavior and enhance its tensile response. Thus, steel fibers came into use due to their advantage in controlling cracks and enhance the tensile behavior of concrete. In this study, the behavior and improvement in flexural tensile strength and strain capacity of ultra-high-performance cement-based composites (UHP-CC) were investigated. Two main variables were examined, namely the content of silica fume and steel fibers with percentages of (0%, 10%, 20% and 30%) and (0%, 1%, 2% and 3%) respectively. The experimental results show that, in the non-fibrous UHP-CC matrix, after the first crack initiation, the inclusion of steel fibers upgrades the behavior of the matrix from brittle to a plastic one and the specimen with a 1% steel fibers ratio failed immediately after crack initiation showing no possible occurrence of strain hardening or multiple cracking. In UHP-CC specimens with steel fibers of more than 1% the tensile failure was more ductile and accompanied by the development of the main crack and many multiple secondary cracks. it was found that the load increased even after the cracks initiation (strain hardening behavior) and thereafter showed gradual declination. It is revealed that after the peak point, one of the cracks widens and becomes critical, which defines the onset of crack localization showing no more development of cracks. Under increased deformation, the critical crack will open describing the stage of fibers pull-out. It was observed that the increase of the ratio of steel fibers in the range of (0% - 3%) caused a significant increase in flexural tensile strength by 244%, whereas the increase in compressive strength was only 12%.

Key words: flexural tensile strength, ultra-high performance, steel fiber, strain hardening, ductility

INTRODUCTION

In the field of concrete science, several technological developments were amassed to produce an advanced cementitious composite ultra-high-performance cementitious-composite, UHP-CC. This type of concrete is considered as a high-strength fiber-reinforced cementitious composite with discontinuous pore structures and improved durability. It has a remarkably low water-to-cementitious materials ratio with an improved granular gradation. UHP-CC has significantly enhanced tensile strength before cracking initiating and after cracking. This enhanced tensile strength is attained by the indiscriminately oriented steel fibers which act as a micro-level reinforcement that increases tensile strength, energy absorption, ductility, and crack control characteristic. After cracking has occurred, the steel fibers can sustain extra tensile loading. This feature can remain present until the fibers are pulled out and the section is severed [1-4]. Laboratory investigations on structural members have evidently shown that UHP-CC components can demonstrate tensile properties that exceed those of conventional and fiber-reinforced concretes [5-8]. Numerous researchers have tried developing the strategies of testing in order to evaluate the tensile strength of fiber reinforced concrete (FRC). These test strategies consist of both direct and indirect evaluation. Some of these tests were standardized [1]. As illustrated in the Japanese Concrete Institute (JCI), specifically Standard JCI-S-003-2007, the method adopted by this standard emphasizes only the curvature curve of bending moment of fiber-reinforced cementitious composites [9]. The method depends on the mensuration of the bending moment-curvature and applied load through flexure testing. The utilized procedure to acquire the stress–strain relationship of the examined materials was a simplified inverse analysis. Figure 1 shows a comparison between the actual stress-strain behavior and the tensile strength and ultimate tensile strain determined by the above-mentioned method. JCI Standard JCI-S-003- considered the evaluated tensile strength and strain determined by this technique to be corresponding to the maximum point tensile stress and strain determined by uniaxial tension test [9]. The inverse analysis is based on the strain measurement method, which was developed by Baby et al., and based on the applied load and the strain Measured in the middle of the bottom flange throughout a flexure test, the stress– strain law of the tested material can be obtained. Based on the equilibrium of forces and moments in a section analysis for each value of mid-span strain and equivalent bending moment, the experimental bending moment and mid-span strain curve is transformed to a tensile stress–strain curve [11].

**11608@uotechnology.edu.iq*

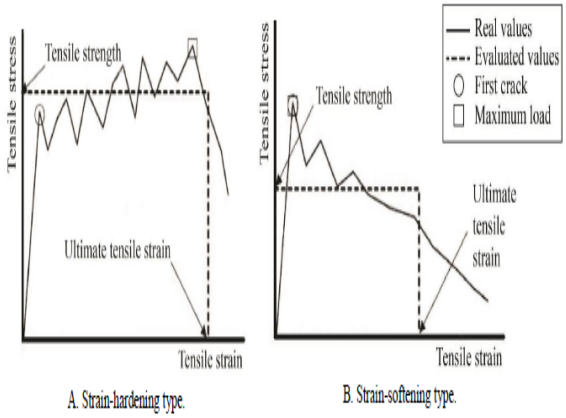

Figure 1: Tensile stress–strain curves (real and evaluated) [10]

AIM OF RESEARCH

The improved tensile strength and high toughness of UHP-CC can be pointed out as its most advantageous features. To enable the material to be fully exploited, tensile behavior must be taken into consideration in the design. This means that the resistance models for ordinary concrete (OC), high strength concrete (HSC) or fiber reinforced concrete (FRC) elements cannot be applied directly. The present research is devoted to determining the fundamental tensile behavior of UHP-CC which is a fundamental aspect of a structural design. The results of this research will assist to clarify and add useful information about tensile behavior and ductility of UHP-CC, which is essential in modeling, analysis, and design of UHP-CC structures.

EXPERIMENTAL PROGRAM

Designation of Specimens

Eight UHP-CC mixes were used in the present research to investigate the tensile stress-strain response of UHP-CC. The two variables considered in the preparation of these eight mixes were the volumetric percentages of the steel fiber (0, 1, 2, and 3%) and silica fume content (0, 10, 20, and 30%). Accordingly, two different groups of mixes were designed as listed in Table 1;

Group 1: MF0, MF1, MF2, MF3

M: mix.

F: fibers volumetric ratio (as a ratio of the mix volume)

In this group, the silica fume content was 25%.

Group 2: MS0, MS10, MS20, MS30

M: mix.

S: silica fume content (as partial replacement of cement weight)

In this group, the steel fibers volumetric ratio was 2%.

Table 1: Mix proportions for the specimens produced in this study

Group	Specimen designation	Cement (kg/m^3)	Sand (kg/m^3)	Silica fume %	Silica fume (kg/m^3)	Steel fiber Vf %	Steel fiber (kg/m^3)	w /c Ratio
1	MF0	750	1000	25%	250	0%	-	0.2
	MF1	750	1000	25%	250	1%	78	0.2
	MF2	750	1000	25%	250	2%	156	0.2
	MF3	750	1000	25%	250	3%	234	0.2
2	MS0	1000	1000	0%	-	2%	156	0.2
	MS10	900	1000	10%	100	2%	156	0.2
	MS20	800	1000	20%	200	2%	156	0.2
	MS30	700	1000	30%	300	2%	156	0.2

Materials Used

Eight batches were prepared in this study using sulfate resisting Portland cement (Type-V), natural very fine sand (maximum particle size is 600μm), densified silica-fume, polycarboxylate superplasticiser (PC 200), produced and supplied by PAC Technologies Company, and hooked steel fibers as shown in Figure 2. The steel fibers properties are presented in Table 2.

Figure 2: The steel fibers used in the present study

Table 2: Steel fibers properties

Description	Length, mm	Diameter, mm	Tensile strength, MPa	Density, kg/m3	Aspect ratio
Hooked end	30	0.5	1280	7800	60

Mixing, Casting, and Curing Procedures

A rotary mixer of 0.1 m3 was utilized to produce all UHP-CC. The time consumed for preparing one batch, calculated from the time of adding water to the mix until adequate flowability is achieved, was in the range of 10-15

minutes. UHP-CC specimens were cast in layers, and each layer was compacted using a table vibrator. Then, the top surface of each specimen was levelled. After that, all specimens were covered by polythene sheets to prevent moisture loss.

Testing of specimens

- Cylindrical specimens (100×200) mm were used for the purpose of calculating the compressive strength (f'c) complying with ASTM-C39 [12]. A testing machine of 2000 kN capacity was used to perform this test. For each mix, the value of the average of each three specimens was considered.
- Prismatic specimens (100x100x400) mm were used for the flexural tensile (ft) and the tensile stress-strain curves testing. Each specimen was examined as a simple beam with a span length of 300 mm under third-point loading according to ASTM-C78 [13]. A testing machine of 2000 kN capacity was also used to perform this test. At each value of the applied load (P), the corresponding tensile strain was measured using electrical resistance strain gauge attached in the middle of the specimen bottom flange over a gauge length of 30 mm, as shown in Figure 3.

Figure 3: Electrical resistance strain gage attached at the mid-section of the specimen

The load from the load cell and the strain from the strain gauge have been used to establish the tensile tress–strain response for each specimen at age 28 days. The electrical resistance strain gage and the strain gage indicator used in this study are shown in Figure 4.

begin with a steep ascending part up to the first cracking point followed by a strain hardening portion (an increase in strain under increasing load) where multiple cracking develops. At the end of the strain hardening part (the peak point), one of the cracks widens and becomes critical, which defines the start of crack localization. Thereafter the tensile resistance decreases showing no more development of cracks. Under increased deformation, the critical crack will be open describing the fibers pull-out stage. Figures (5a, 5b) show that for the UHP-CC specimen with 0% and 1% steel fibers the ascending portion of the stress-strain curve has a slope similar to that of specimens with 2% and 3% steel fibers, but it terminates at the first cracking point showing no possible occurrence of strain hardening or multiple cracking. The descending part of the tensile stress-strain curve was seen to vanish in a non-fibrous specimen while it showed a small tail in the specimen with 1% steel fibers. After failure, it turns out that there is one big crack accompanying fibers, which play a significant role in bridging the crack faces. Due to the fibers bridging mechanism, UHP-CC can provide superior performance compared to nonfibrous UHP-CC, especially under tension. Figure 6 presents a typical crack pattern after the flexural test.

Figure 4: Electrical resistance strain gage and strain gage indicator

TEST RESULTS

The experimental test results for UHP-CC mixes are presented in Table 3, and the typical tensile stress-strain response in the flexural test is plotted in Figure 5. The results show that the curves of tensile stress-strain of UHP-CC specimens with steel fibers more than 1%

Table 3: Test results

Group	Specimen designation	Steel fiber %	Silica fume%	ft (MPa)	The increase in ft %	εtp*	f'c (MPa)	The increase in f'c %
1	MF0	0%	25%	10.43	0	0.000137	127.7	0
	MF1	1%	25%	17.24	65	0.000149	134.5	5
	MF2	2%	25%	26.81	157	0.002951	140.7	10
	MF3	3%	25%	35.89	245	0.003918	142.4	12
2	MS0	2%	0%	23.84	0	0.002814	110.1	0
	MS10	2%	10%	24.39	2	0.002846	129.6	18
	MS20	2%	20%	25.84	8	0.003014	138.5	26
	MS30	2%	30%	27.41	15	0.002920	148.7	35

* εtp: The strain at peak flexural tensile strength (ft)

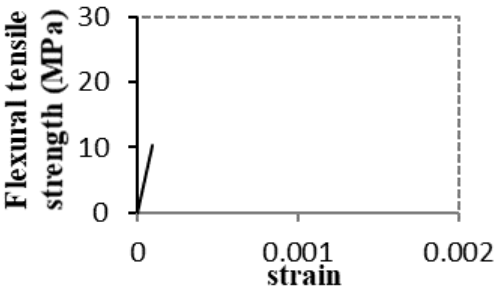

(a) MF0

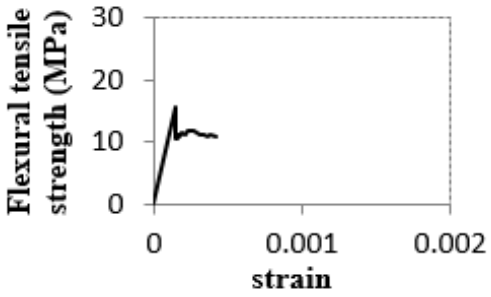

(c) MF2

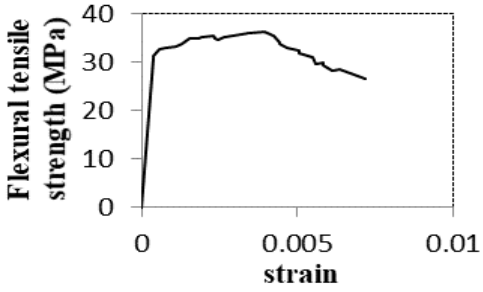

(d) MF3

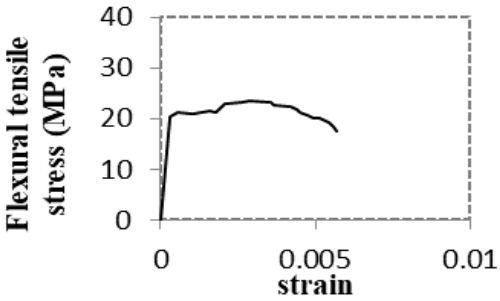

(f) MS10

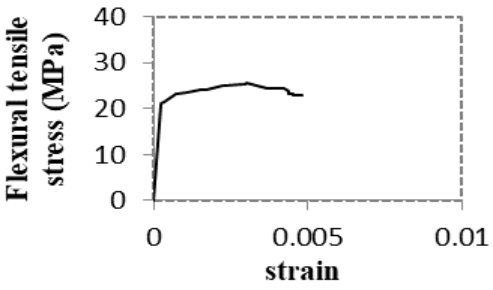

(g) MS20

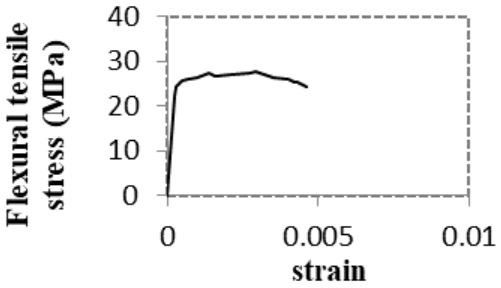

(h) MS30

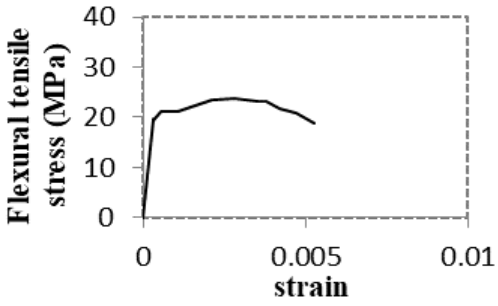

(e) MS0

Figure 5: UHP-CC flexural tensile response

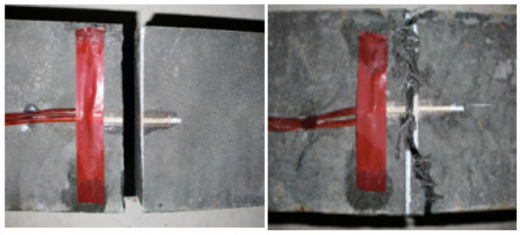

Figure 6: Typical crack pattern after the flexural test

Tensile response of UHP-CC with different steel fibers volume fractions (Vf)

The experimentally obtained tensile response in flexure for UHP-CC with different fiber volume fractions is shown in Figure 7. Results indicated that the non-fibrous UHP-CC specimen (MF0) and the specimen with 1% steel fibers ratio (MF1) failed immediately after crack initiation and the load was found to decrease rapidly, While UHP-CC specimens with 2% and 3% steel fibers showed

different tensile behavior. In these specimens, the tensile failure was more ductile and accompanied by the development of the main crack and many multiple secondary cracks. The load was found to increase even after crack initiation (strain hardening behavior) and thereafter showed gradual declination. This behavior can be attributed to the ability of steel fibers to arrest and slow down the process of micro-cracks propagation.

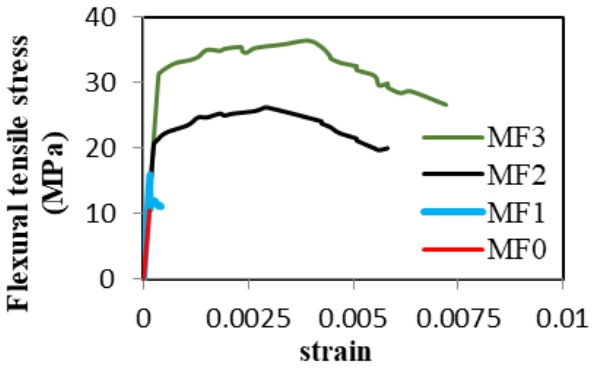

Figure 7: Flexural tensile response with respect to fiber volumetric ratio

It can be observed from table 3 and figure 7 that by increasing the steel fibers volumetric ratio from 0% to 3%, the area under the stress–strain curves significantly increased, and also caused a considerable increase in both the flexural tensile strength from 10.43 to 35.89 MPa and its strain from 0.000137 to 0.003918. This behavior can be attributed to the ability of steel fibers to bridge matrix crack and higher energy is needed for crack propagation. Generally, hooked steel fibers significantly increase the tensile strength as the geometry of the hooked fibers affects the development of the bond between the fibers and the matrix and requires more energy to extract the fiber from the matrix [14].

Tensile response of UHP-CC with different silica fume content

Table 3 and Figure 8 presents a comparison of UHP-CC tensile response with different silica fume content. It is revealed that the influence of silica fume content on the flexural tensile strength is lower than that on the compressive strength. Increasing the silica fume content from 0% to 30% led to an increase in flexural tensile strength (ft) of 15%, while the percentage of increase in compressive strength (f'c) was 35%. These beneficial effects of silica fume can be attributed to the pozzolanic reaction of the particles of silica fume and their physical effect resulting from the improved particle packing. This behavior improves the microstructure of the UHP-CC [15].

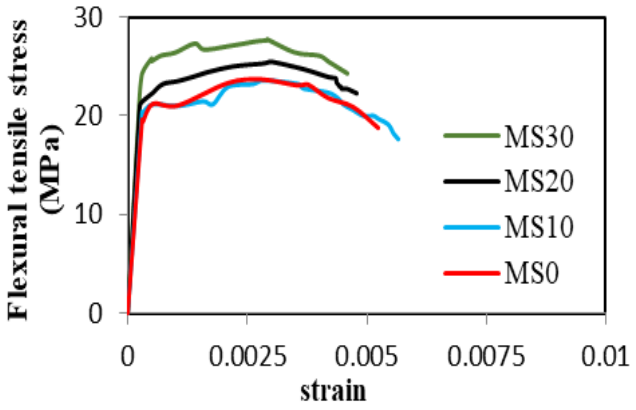

Figure 8: Flexural tensile response with respect to silica fume content

CONCLUSION

Many conclusions were drawn based on the experimental results obtained by the present study. These conclusions are listed as the following:

1. After the first crack forming, the steel fibers utilization changes the nature of the non-fibrous UHP-CC from brittle to a composite mass with a plastic behavior. Besides, the presence of steel fibers provided an extended plastic range for the tensile stress-strain curve with higher peak strength and larger ductility.
2. Results indicated that the non-fibrous UHP-CC specimen and the specimen with 1% steel fibers ratio failed immediately after crack initiation and the load was found to decrease rapidly showing no possible occurrence of strain hardening or multiple cracking.
3. UHP-CC specimens with steel fibers more than 1% showed different tensile behavior. In these specimens, the tensile failure was more ductile and accompanied by the development of the main crack and many multiple secondary cracks. The load was found to increase even after crack initiation (strain hardening behavior) and thereafter showed gradual declination.
4. After the end of the strain hardening portion (the peak point), one of the cracks widens up and becomes critical defining the onset of crack localization showing no more development of cracks. The critical crack will open under increased deformation describing the stage of fibers pull-out.
5. The most noteworthy result for increasing the steel fibers ratio from 0% to the three selected values (1%, 2%, and 3%) was the enhancement in both the flexural tensile strength and its corresponding strain. This was observed by the percentage of increment in flexural tensile strength compared to the non-fibrous specimens were 65%, 157%, and 244% respectively. While the percentages of increment in the compressive strength (f'c) compared to the non-fibrous specimens were 5%, 10%, and 12% respectively.

6. It is revealed that the influence of silica fume content on flexural tensile strength is less pronounced than that on compressive strength. Increasing silica fume content from 0% to 30% resulted in an increase in flexural tensile strength (ft) by 15%, whereas the percentage of the compressive strength (f′c) increase was 35%.

The results of this research can be used to study the direct shear behavior of UHP-CC reinforced elements using a pre-selected shear plane in concrete members named push-off specimens that needed to study the behavior of reinforced UHP-CC members subjected to in-plane loadings such as corbels, wall to foundation connections, and panels.

REFERENCES

1. Graybeal, B. A., and Baby, F., Tension testing of ultra-high performance concrete (No. FHWA-HRT-17-053). Federal Highway Administration, Office of Infrastructure Research and Development, United States, (2019). Retrieved from https://www.researchgate.net/publication/331651550
2. Graybeal, B.A., Structural behavior of ultra-high performance concrete prestressed I-girders (No. FHWA-HRT-06-115). Federal Highway Administration, Office of Infrastructure Research and Development, United States, (2006). Retrieved from https://www.researchgate.net/publication/313505596
3. Danha, L.S. Tensile Behavior of Reactive Powder Concrete. M.Sc. Thesis, University of Technology, Baghdad, Iraq, (2012).
4. Al-Hassani, H. M., Khalil, W. I., and Danha, L. S. “Proposed model for uniaxial tensile behavior of ultra high performance concrete.” Engineering and Technology Journal, Vol. 33, No. 1, (2015), 61-77. Retrieved from https://www.researchgate.net/publication/325063976
5. Fischer, G., and Li, V. C. “Effect of fiber reinforcement on the response of structural members.” Engineering Fracture Mechanics, Vol. 74, No. (1-2), (2007), 258-272. Retrieved from https://doi.org/10.1016/j.engfracmech.2006.01.027
6. Pansuk, W., Nguyen, T. N., Sato, Y., Den Uijl, J. A., and Walraven, J. C. “Shear capacity of high performance fiber reinforced concrete I-beams.” Construction and Building Materials, Vol. 157, (2017), 182-193. Retrieved from https://doi.org/10.1016/j.conbuildmat.2017.09.057
7. Danha, L. S., Abdul-hussien, Z. A., Abduljabbar, M. S., and Yassin, L. A. G. “Flexural behavior of hybrid ultra-high-performance concrete.” IOP Conference Series: Materials Science and Engineering, Vol. 737, No. 1, (2020), 1-9. DOI: 10.1088/1757-899X/737/1/012008
8. Baby, F., Billo, J., Renaud, J. C., Massotte, C., Marchand, P., Toutlemonde, F., Simon, A., and Lussou, P. “Shear resistance of ultra high performance fibre-reinforced concrete I-beams.” FraMCoS7, (2010), 1411-1417. Retrieved from http://madis-externe.ifsttar.fr/exl-php/DOC0001986
9. Technical Committee JCI. Method of test for bending moment-curvature curve of fiber-reinforced cementitious composites. (2007) Retrieved from http://www.jcinet.
10. Japan Concrete Institute JCI. “Method of test for bending moment-curvature curve of fiber-reinforced cementitious composites.” Journal of Advanced Concrete Technology, Vol. 4, No. 1, (2006), 73-78. DOI: https://doi.org/10.3151/jact.4.73
11. Baby, F., Graybeal, B., Marchand, P., and Toutlemonde, F. “Proposed flexural test method and associated inverse analysis for ultra-high-performance fiber-reinforced concrete.”ACI Materials Journal, Vol. 109, No. 5, (2012) 545-556. Retrieved fromhttps://www.concrete.org/publications/acimaterialsjournal.aspx
12. American Society of Testing and Materials ASTM C39, Standard test method for compressive strength of cylindrical concrete specimens. (2015).
13. American Society of Testing and Materials ASTM C78, Standard test method for flexural strength of concrete (using simple beam with third-point loading). (2015).
14. Al-Hassani, H .M., Khalil, W. I.,and Danha, L. S. “Prediction of the nominal bending moment capacity for plain and singly reinforced rectangular RPC beam sections.” Engineering and Technology Journal, Vol. 33, No. 5, (2015), 1113-1130. Retrieved https://www.researchgate.net/publication/325063802
15. Dubey, A., and Banthia, N. “Influence of high-reactivity metakaolin and silica fume on the flexural toughness of high- performance steel fiber reinforced concrete.” Materials Journal, Vol. 95, No. 3, (1998), 284-29. Retrieved from https://www.concrete.org/publications/acimaterialsjournal.aspx

Paper submitted: 20.05.2021.
Paper accepted: 12.08.2021.